

Research Article

Dye-Sensitized Nanocrystalline ZnO Solar Cells Based on Ruthenium(II) Phendione Complexes

Hashem Shahroosvand,¹ Parisa Abbasi,¹
Mohsen Ameri,¹ and Mohammad Reza Riahi Dehkordi²

¹ Chemistry Department, University of Zanjan, Zanjan, Iran

² Laser Research Institute, Shahid Beheshti University, Evin, Tehran, Iran

Correspondence should be addressed to Hashem Shahroosvand, shahroos@znu.ac.ir

Received 24 July 2011; Revised 20 September 2011; Accepted 23 September 2011

Academic Editor: Newton Martins Barbosa Neto

Copyright © 2011 Hashem Shahroosvand et al. This is an open access article distributed under the Creative Commons Attribution License, which permits unrestricted use, distribution, and reproduction in any medium, provided the original work is properly cited.

The metal complexes $(\text{Ru}^{\text{II}}(\text{phen})_2(\text{phendione}))(\text{PF}_6)_2$ (1), $[\text{Ru}^{\text{II}}(\text{phen})(\text{bpy})(\text{phendione}))(\text{PF}_6)_2$ (2), and $(\text{Ru}^{\text{II}}(\text{bpy})_2(\text{phendione}))(\text{PF}_6)_2$ (3) (phen = 1,10-phenanthroline, bpy = 2,2'-bipyridine and phendione = 1,10-phenanthroline-5,6-dione) have been synthesized as photo sensitizers for ZnO semiconductor in solar cells. FT-IR and absorption spectra showed the favorable interfacial binding between the dye-molecules and ZnO surface. The surface analysis and size of adsorbed dye on nanostructure ZnO were further examined with AFM and SEM. The AFM images clearly show both, the outgrowth of the complexes which are adsorbed on ZnO thin film and the depression of ZnO thin film. We have studied photovoltaic properties of dye-sensitized nanocrystalline semiconductor solar cells based on Ru phendione complexes, which gave power conversion efficiency of (η) of 1.54% under the standard AM 1.5 irradiation (100 mW cm^{-2}) with a short-circuit photocurrent density (J_{sc}) of 3.42 mA cm^{-2} , an open-circuit photovoltage (V_{oc}) of 0.622 V, and a fill factor (ff) of 0.72. Monochromatic incident photon to current conversion efficiency was 38% at 485 nm.

1. Introduction

Dye-Sensitized Solar Cells (DSSCs) [1, 2] are attracting lot of interest because of their low cost and high efficiency. Many researchers have made efforts to modify the cell from various aspects to improve the DSSC efficiency. It is generally accepted that the dye-sensitized reaction step and electron injection step between the electrodes and the excited adsorbed dye are the key steps to control DSSCs efficiency [3–5]. For the optimization of the DSSCs components, that is, the different oxide semiconductor, the dye sensitizer and the electrolyte, exactitude in reporting the experimental procedures used is indispensable in order to compare the data between the many different laboratories active in this field [6, 7]. Titanium dioxide advantages for sensitized photochemistry and photoelectrochemistry including a low-cost, widely available, nontoxic, and biocompatible material, and as such is even used in health care products as well as domestic applications such as paint pigmentation [8, 9]. But, TiO_2 films have a significant limitation that makes it

difficult to grow on a substrate with controlled structure. This may prevent further development of DSSCs with TiO_2 films. One-dimensionally ordered structures of metal oxides, such as rods or wires, will greatly improve DSSCs efficiency [10, 11]. Therefore, extensive attention has been focused on looking for the suitable substitute for TiO_2 . Among these candidates, ZnO has been expected to be comparable to TiO_2 because of its higher electronic mobility, similar energy level of the conduction band [12, 13], conductive crystal structure due to the anisotropic growth [14, 15], and its potential in high-area film morphologies [16]. ZnO is a versatile material that has a diverse group of morphologies; compared with nanocrystalline particle ZnO films, ZnO films containing vertically aligned nanorods ZnO film favor the electron transport due to the smoother electron transport channels and longer electron diffusion length [17–19].

However, the DSSC efficiency based on ZnO is much lower compared to that based on TiO_2 . One of the reasons for the relative low DSSC performance is due to the precipitation of the sensitizing dye with Zn cations on ZnO films [20].

On the other hand, much of the research in dye chemistry is devoted to the identification and synthesis of dyes matching the solar emission spectrum, while retaining stability in the photoelectrochemical environment. The anchoring groups of the dye ensure that it spontaneously assembles as a molecular layer upon exposing the oxide film to a dye solution. The best photovoltaic performance both in terms of conversion yield and long-term stability has so far been achieved with polypyridyl complexes of ruthenium and osmium. Sensitizers having the general structure $ML_2(X)_2$ where L stands for 2,2-bipyridyl-4,4-dicarboxylic acid, M is Ru or Os, and X presents a halide, cyanide, thiocyanate, acetyl acetonate, thiocarbamate, or water substituent, are particularly promising [21]. Several reports have already discussed the results obtained for ruthenium complexes having noncarboxylic acid anchoring group, such as phosphonic and catechol [22–28]. Among various kinds of polypyridyl ligands, 1,10-phenanthroline-5,6-dione (phendione) is a versatile ligand for the assembly of metal organic materials [29–32]. This ligand has the ability to form stable complexes with a wide variety of metal ions and carries an o-quinone moiety. Metal complexes of this ligand potentially allow for the variation and control of redox properties over a wide range as well as the fine-tuning of potentials [33].

We reported a new class of complexes, $(M(\text{phendione})(L_1)(L_2))$, where $M = \text{Os(II)}, \text{Ru(II)}, \text{Cu(I)}$, $L_1, L_2 = \text{phen or bpy}$ as photosensitizers based on TiO_2 , MoO_2 nanoparticles [34–36]. In this manuscript we design a new class of ruthenium phendione complexes, which have the carbonyl ligand as anchoring group based on ZnO nanoparticle. The dye-anchored ZnO surface was characterized by FT-IR, UV-visible, and AFM. The photovoltaic performances of phendione complexes based on ZnO have been studied.

2. Experimental

2.1. Materials and Physical Measurements. All chemicals and solvents were purchased from Merck & Aldrich and used without further purification. UV-Vis spectra were recorded on an analytikjena SPECORD S1000 spectrometer with photodiode array detector. FT-IR spectra were recorded on a Shimadzu IR instrument, using KBr pellets. Atomic force microscopy (AFM) images of the samples were measured using an SPM (Digital Instruments, DME Software, Mahar Fan Abzar Co.) in the contact mode and stylus profilometry (Alpha-step 500). All scans were taken at room temperature in air. Imaging was performed using pyramidally shaped silicon nitride tips ($4\ \mu\text{m}$ base, $4\ \mu\text{m}$ height, aspect ratio approximately 1 : 1, radius $<50\ \text{nm}$) on silicon nitride cantilevers (typical spring constant = $0.032\ \text{N/m}$). In all the AFM scans, there are 512×512 data points across the areas of the scan and contact scans were made. The AFM is the preferred measurement technique as the force between the probe and the surface is much smaller (typically $10\text{--}9\ \text{N}$) than for the stylus profilometer ($150\ \text{mN}$), and the tip has a much smaller radius of curvature (AFM $0.05\ \mu\text{m}$, profilometer $12.5\ \mu\text{m}$). Therefore the AFM results are more representative of the surface topography than those of the profilometer and also

have a greater sensitivity, with the ability to measure height variations of $0.1\ \text{nm}$ with a horizontal resolution of $<4\ \text{nm}$.

Photoelectrochemical measurements employed the dye-sensitized ZnO film incorporated into a thin-layer sandwich-type solar cell. A light-reflecting counter electrode was employed, consisting of a conducting zinc oxide-coated glass onto which a $2\ \mu\text{m}$ thick Pt mirror had been deposited by sputtering. The counter electrode was placed directly on top of the dye-coated transparent ZnO film, supported by the conducting glass sheet. Both electrodes were clamped tightly together. The dye-coated ZnO film was illuminated through the conducting glass support, a 1000 W Xe lamp. The short-current measurement was performed using a potentiostat model CMBP-1. The intensity of the light was calibrated using a model OM-100IC radiometer/photometer.

2.2. Synthesis

2.2.1. Preparation of Ru (II) Phendione Complexes. The Complexes $(\text{Ru}^{\text{II}}(\text{phen})_2(\text{phendione}))(\text{PF}_6)_2$; (Anal. Calcd: C, 44.96; H, 2.30; N, 8.73; found: C, 44.92; H, 2.29; N, 8.70) and $(\text{Ru}^{\text{II}}(\text{bpy})_2(\text{phendione}))(\text{PF}_6)_2$ (Anal. Calcd: C, 42.06; H, 2.50; N, 9.19; found: C, 44.89; H, 2.49; N, 9.15); were synthesized following the procedure of Goss and Abruna [29]. The $(\text{Ru}^{\text{II}}(\text{phen})(\text{bpy})(\text{phendione}))(\text{PF}_6)_2$ (Anal. Calcd: C, 43.55; H, 2.36; N, 8.96; found: C, 43.50; H, 2.32; N, 8.90) complex was prepared, using the same procedure except using 1 mol phen and 1 mol bpy instead of 2 mol phen.

2.2.2. Preparation of ZnO Nanoparticle Film. Fisher microscope glass slides were used as substrates; ZnO-coated glass films already were boiled in deionized (DI) water for 0.5 hour, then ultrasonically cleaned in acetone and alcohol solution (1 : 1 v : v) for 1 hour, and finally dried in oven at 100°C for 3 hours.

Film substrates were secured, conductive side up to a piece of white paper with electrode surface. The cellophane tape served to mask an area of the film for ohmic contact to the contactive glass. Typically the ZnO, geometric area was $1\ \text{cm}$.

After the pretreatment, these slides were ready for the following chemical bath deposition. The chemical bath was prepared from 15 mL of 0.15 mol/L zinc acetate dihydrate ($\text{Zn}(\text{CH}_3\text{COO})_2 \cdot 2\text{H}_2\text{O}$) methanol solution. Following deposition for 30 hours at 60°C , the as-synthesized films were annealed at 200°C for 5 min and then at 450°C for 15 min [44].

2.2.3. Surface Attachment of Dyes. The Ru phendione complexes were dissolved in dehydrated ethanol with a concentration of 0.25 M. ZnO nanoparticle film was immersed into the solution of each complex and maintained at 40°C for over 18 h to coordinate complex on the ZnO surface [45]. During this time the film surface charges to the brown that is the color of the attached dyes. After adsorption, ZnO films with Ru-phendione dyes were withdrawn from the solution and dried in air.

3. Results and Discussion

The Chemical structures of synthesized complexes were shown in Figure 1.

3.1. FT-IR and UV-Vis Absorption Measurements. The Fourier transform IR (FT-IR) spectroscopy has been shown to be a powerful tool for extracting structural information of the molecules adsorbed onto a ZnO surface.

The (FT-IR) spectra of complexes measured as a powder show the most prominent band at approximately 1700 cm^{-1} in all of the complexes which is assigned to C=O stretching wave number of the coordinated phendione ligand [46]. In case of the attachment of the dye molecules on ZnO, the oxygen of carbonyl group would be coordinated to ZnO; therefore, we expected the C=O stretch band to be shifted to lower wavelength.

FT-IR spectra of phendione complexes (1) and phendione dye adsorbed ZnO films (2) are shown in Figure 2. Adsorption band at 1700 cm^{-1} in spectrum (1) and 1670 cm^{-1} in spectrum (2) corresponds to the C=O and C–O stretching from carbonyl group before and after dye adsorption on ZnO surface, respectively. FT-IR spectrum of dye-adsorbed ZnO films (2) also was shown Zn–O stretching at 530 cm^{-1} .

The diffuse reflectance IR spectra of complexes as shown above anchored to ZnO film are listed in Table 1.

The possible binding modes for Ru polypyridine complexes containing carbonyl groups on ZnO surface are shown in Scheme 1.

If the difference between the carbonyl group stretching mode band in the adsorbed state is less than that in the free solid state, then, the anchoring mode is either bridging bidentate (II) or chelation (III), and if the opposite applies, then, the anchoring mode is unidentate.

The unidentate coordination of the carbonyl group removes the equivalence of the two oxygen atoms, resulting in an ether type of bond formation between the carbonyl group and the ZnO surface and also free carbonyl in dye.

The FT-IR spectra of the adsorbed Ru polypyridine complexes (1)–(3) on ZnO film do not exhibit typical free carbonyl stretching modes; thus this type of coordination can be ruled out, leaving only two possibilities, bridging bidentate mode (II) or chelation mode (III).

Unidentate mode (I) is also reported by Li et al. [23] for phendione complexes. In this work, they suggested that the C=O stretch band observed at a lower wavelength than that of the phendione complexes in KBr pellets was ascribed to the shift caused by the contribution in the formation of the unidentate bond between the dye molecules and TiO_2 surface. Comparing our obtained data from IR spectra (520 cm^{-1}) with Zn–O band in the chelating mode (III) and the bridging-bidentate mode (II) available in reported data [46] suggests that our results are closer to chelating mode (III) and the bridging-bidentate mode is unexpected. Therefore, the carbonyl groups are probably bound to the ZnO surface via a chelating mode (III).

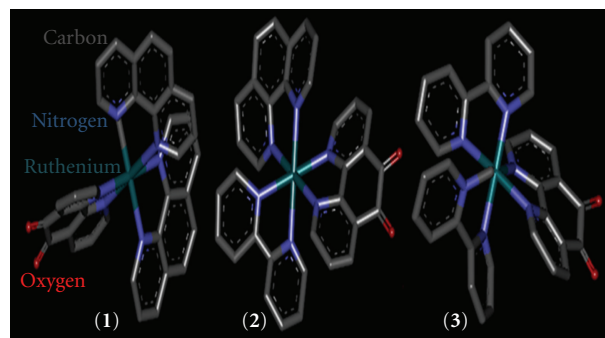


FIGURE 1: The chemical structures of synthesized complexes ($\text{Ru}^{\text{II}}(\text{phen})_2(\text{phendione})^{2+}$ (1), ($\text{Ru}^{\text{II}}(\text{phen})(\text{bpy})(\text{phendione})^{2+}$ (2), and ($\text{Ru}^{\text{II}}(\text{bpy})_2(\text{phendione})^{2+}$ (3).

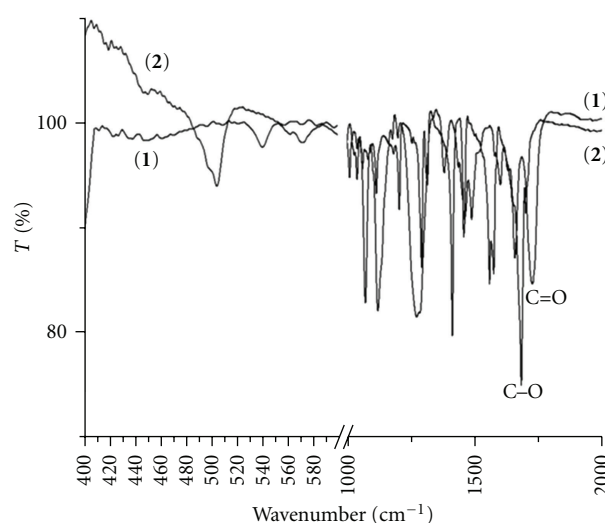


FIGURE 2: FT-IR spectra of phendione complexes (1) and phendione complexes adsorbed ZnO films (2).

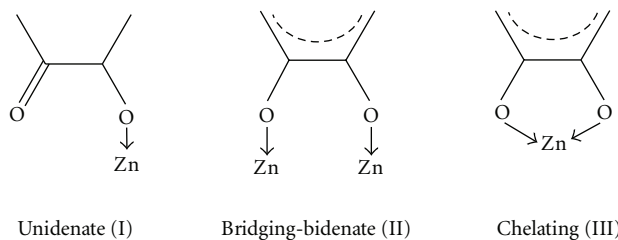
The absorption spectra of the dye based on ZnO nanoparticle are compared with the solution spectra in Figure 3.

These complexes show broad and strong visible bands around 450–470 nm regions due to metal-to-ligand charge transfer (MLCT) transitions. Two distinct absorption bands in the UV region are due to the ligands $\pi \rightarrow \pi^*$ transitions.

As shown in Figure 3, one can observe that the absorption band in visible region is shifted to short wavelength (blue shift) and its intensity is enhanced comparing to the complexes which are not adsorbed to ZnO nanoparticle (Table 2). These results indicate that the charge transfer interaction is responsible for binding the ruthenium complexes on ZnO film. There are reports that when carboxylic acid group as anchoring group is adsorbed on metal oxides, absorption bands shifted to long wavelength (red shift) [10, 11, 47]. On the other hand, when changing from the carbonyl groups to the carboxylic ones, that is, from electron-acceptor to electron-donor, absorption band apparently shifted from short wavelength to long one. The blue shift in UV-vis spectra in the MLCT bands of phendione complexes is already observed [23].

TABLE 1: Electronic^a and Infrared^b data for the dyes^c and dyes on ZnO surface^d.

Dye	MLCT ^c	MLCT ^d	ν (C=O) ^c	ν (C–O) ^d	ν (Zn–O) ^d
(1)	467 (2.4)	420 (3.4)	1700	1670	520 (broad)
(2)	465 (2.3)	420 (3.3)	1702	1667	523 (broad)
(3)	460 (2.3)	415 (3.1)	1697	1665	515 (broad)

^a λ in nm ($\log \epsilon$) in ethanol solution.^b IR data (KBr) in cm^{-1} .

SCHEME 1: The possible binding modes for the carbonyl groups of phendion molecule with ZnO.

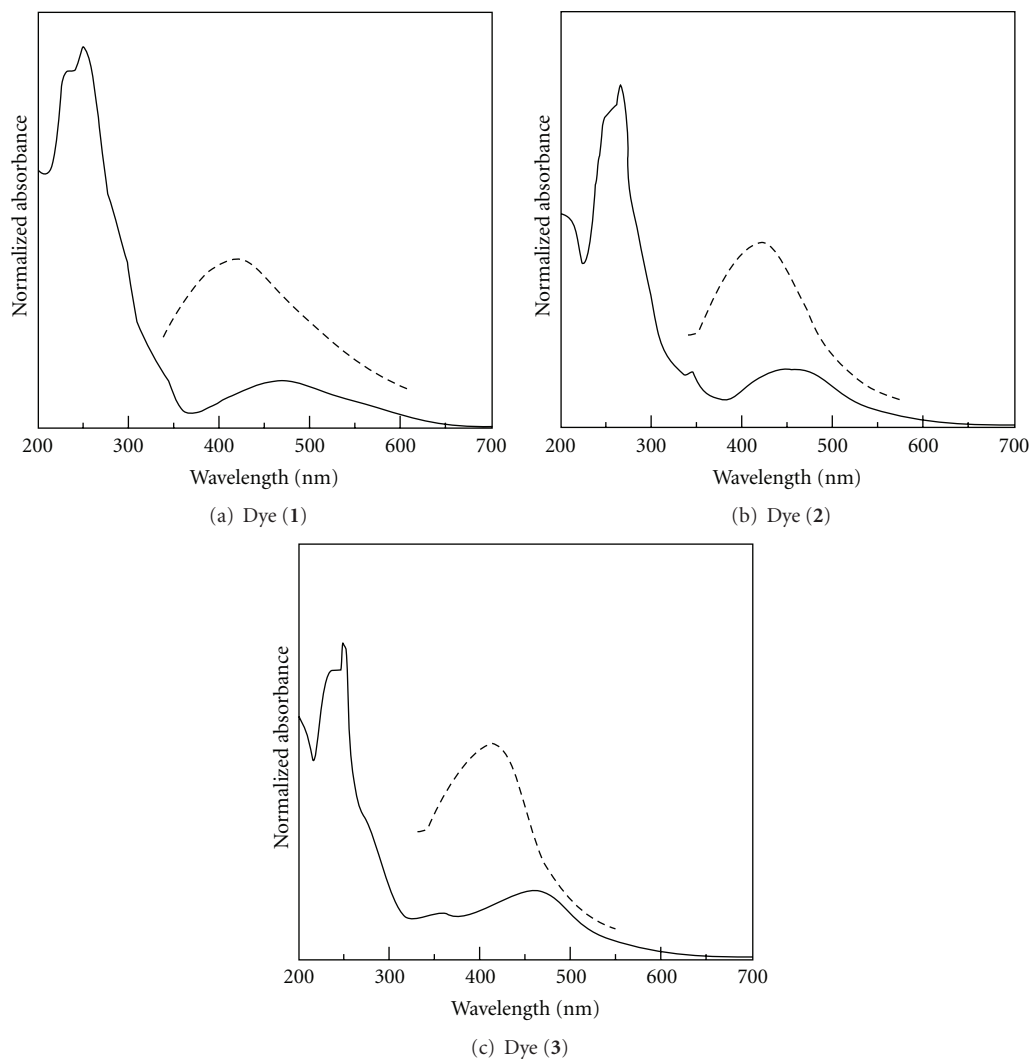


FIGURE 3: Absorption spectra of dye (1) (solid line) in ethanol and adsorbed on ZnO film (dashed line) (a), dye (2) in ethanol (solid line) and adsorbed on ZnO film (dashed line) (b), and absorption spectra of dye (3) (solid line) in ethanol and adsorbed on ZnO film (dashed line) (c).

TABLE 2: Photocurrent performance data obtained with ruthenium photosensitizer with noncarboxylic acid anchoring group ligand [39].

Dye	V_{oc} (V)	I_{sc} (mA cm ⁻²)	IPCE _{max} (%)	ff	η_{cell} (%)		Ref
(Ru(ttp-PO ₃ H ₂)(dmbpy)(NCS))	0.653	4.73	75.6	0.705		TiO ₂	[22]
Ru(bpy-(PO ₃ H ₂) ₂) ₂ NCN ₂	0.490	5	75	0.67		TiO ₂	[40]
(Ru(bpy) ₂ (pySH) ₂)	0.019	0.036	2.9			ZnO	[41]
(Ru(bpy) ₂ (pyS ⁻) ₂)	0.0321	0.045	5.6			ZnO	[41]
(Ru(bpy) ₂ (phendione))PF ₆			34			TiO ₂	[23]
(Ru(bpy) ₂ (phendioxime))PF ₆			27			TiO ₂	[23]
(Ru(bpy) ₂ (NCS))	0.36	1.2		0.5	0.34	TiO ₂	[42]
(Ru(dmbpy) ₂ (bpy-acac))PF ₆	0.487	2.02	0.292			TiO ₂	[43]
(Ru(bpy) ₂ (bpy-CH ₂ COOLi))PF ₆	0.245	0.83	34 ± 5			TiO ₂	[24]
(Ru(phen) ₂ (phendione)) ²⁺	0.622	3.42	38	0.72	1.54	ZnO	Our work
(Ru(phen)bpy)(phendione)) ²⁺	0.619	3.37	36.5	0.71	1.51	ZnO	Our work
(Ru(bpy) ₂ (phendione)) ²⁺	0.618	3.33	36	0.69	1.495	ZnO	Our work

Based on literature [48], if the absorption coefficient of the dye itself can be enhanced, the enhancement of the conversion efficiency of DSCCs will be expected.

The broadening of the absorption band is also beneficial in extending the photoresponse of ZnO. These changes let us use the phendione complexes implanted on ZnO in solar cells.

3.2. Atomic Force Microscopy (AFM) and Scanning Electron Microscopy (SEM) Measurements. The surface analysis of products was further examined with AFM.

A medium-scale image (10 × 10 μm) gathered by AFM on the dried complex (1) adsorbed on ZnO is shown in Figure 4(a).

To clarify the different regions of layered structure, some parts of Figure 4(a) are expanded with different resolution magnitudes and represented in Figure 4(b) (2.47 × 2.47 μm), Figure 4(c) (2.45 × 2.45 μm), Figure 4(d) (1 × 1 μm), Figure 4(f) (348 × 348 nm), and Figure 4(e) (276 × 276 nm).

In all of the zoomed images, one can be ZnO molecules packed in an irregular spongy pattern with nanoporous sizes. The light points of image are shown as adsorbed complex on ZnO nanoparticle film. In fact, light in the topographic images corresponds to a high value of surface free energies. These results indicate that the layered structure is composed of the alternation of adsorbed complex on ZnO and ZnO nanoparticles.

Figures 4(e) and 4(f) represent the zoomed images of Figure 4(d). These images show that the particle size of the adsorbed complex is about 46.5 nm and the size of one of the pores is about 24 nm.

Figure 5 shows Scanning electron microscopy of ZnO nanoparticle before (A) and after absorption with dye (1). The specimen surface in Figure 5(a) appears nanoparticles with about 50 nm. From the SEM image, we can see that the ZnO film is uniform and compact on the glass substrate. In presence of dye (Figure 5(b)), the data gave the surface of ZnO surface with absence of porous and large aggregation of particles. The surface of ZnO film has been covered

with many aggregated particles (Figure 5(b)). Comparing this SEM image with the ZnO film before dye adsorption, we believe that these particles are aggregated phendione dye. It is well known that dye aggregation in ZnO is one of the major problems of the dye adsorption process, which decreases the consequent DSCCs efficiency [13]. One of the main tasks of this work is to solve the dye aggregation problem.

3.3. Photovoltaic Performance. Photovoltaic performance of nanocrystalline oxide semiconductor ZnO solar cells sensitized by phendione complexes photosensitizer under the standard AM 1.5 irradiation (100 mW cm⁻²) is shown in Table 2. Also, photocurrent performance data for ruthenium complexes with noncarboxylic acid anchoring polypyridines, in dye-sensitized solar cell, are listed in Table 2, where J_{sc} is the short-circuit photocurrent density, V_{oc} is open-circuit photovoltage, ff is the fill factor, and η is solar energy to current conversion efficiency.

These semiconductor films were almost transparent because large semiconductor particles were not included as a scattering center. The electrolyte solution was a mixture of 0.6 M DMPIImI, 0.1 M LiI, 0.05 M I₂, and 0.5 M TBP in methoxyacetonitrile.

A typical photocurrent-voltage curve for the (Ru(phen)₂(phendione))²⁺ (1) solar cell under standard AM 1.5 irradiation (100 mW cm⁻²) is shown in Figure 6. Solar energy to electricity conversion efficiency, η , of 1.54% was attained with J_{sc} of 3.42 mAcm⁻², V_{oc} of 0.622 V, and ff of 0.72.

Figure 7 shows monochromatic incident photon to current conversion efficiency with the nanocrystalline ZnO solar cell sensitized by (Ru(phen)₂(phendione))PF₆ (1) with the electrolyte of 0.6 M DMPIImI, 0.1 M LiI, 0.05 M I₂, and 0.5 M TBP in methoxyacetonitrile (solid line). IPCE is represented as a function of wavelength. Ru(deeb)(bpy)₂²⁺/TiO₂ in 0.5 M LiClO₄/0.05 M I₂ electrolyte. The TiO₂ surfaces were pretreated with pH 2 (circles) aqueous solution [37]. Ru(deeb)₂(py)₂/TiO₂ (squares) and Ru(bpy)₂(ina)₂/TiO₂ (triangles) regenerative solar cell in 0.5 M LiI/0.05 M I₂ acetonitrile electrolyte [38] where py is pyridine, ina is

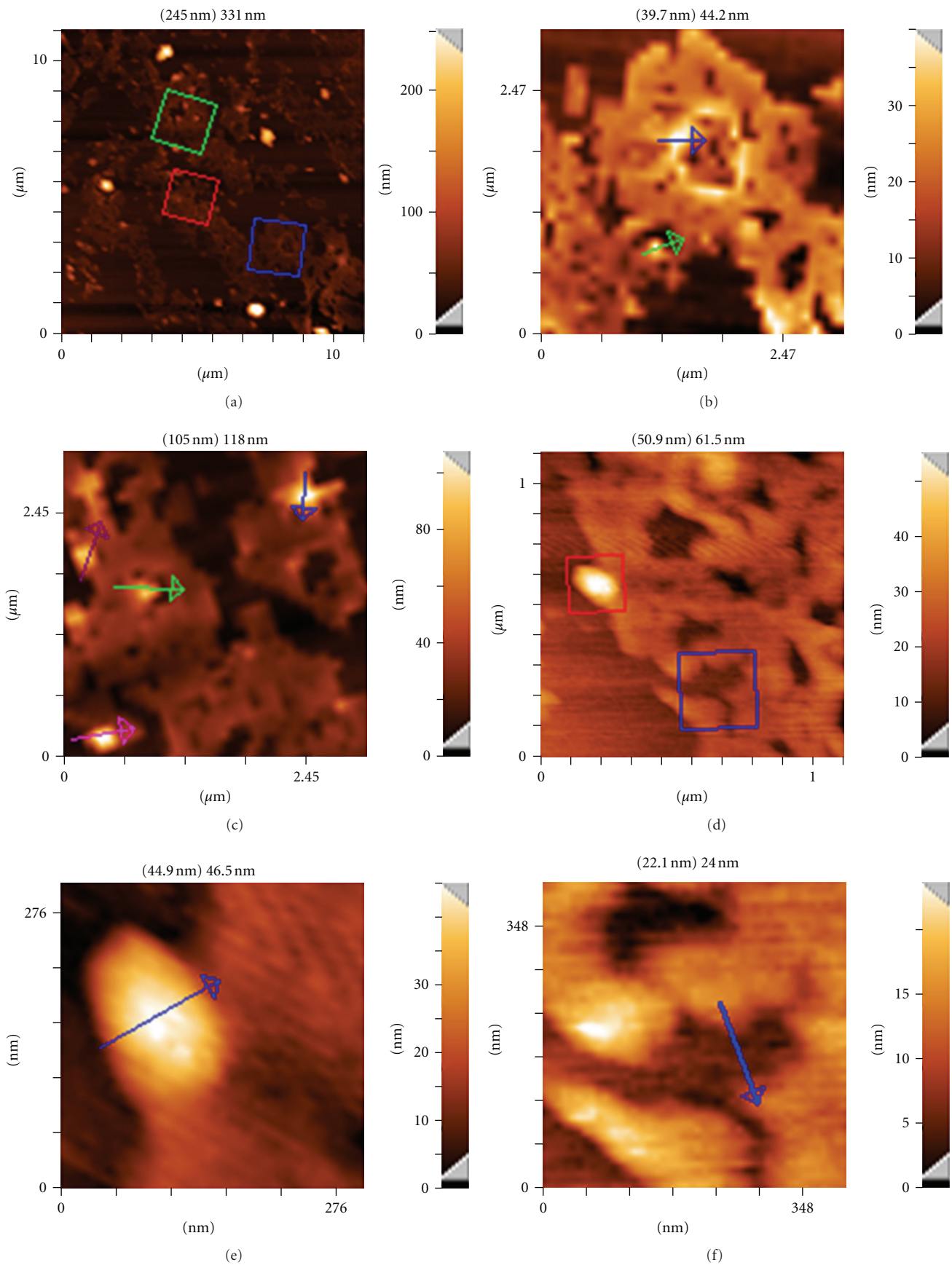


FIGURE 4: AFM topographic images of absorbed phendione complex (1) on the thin film of ZnO nanoparticles.

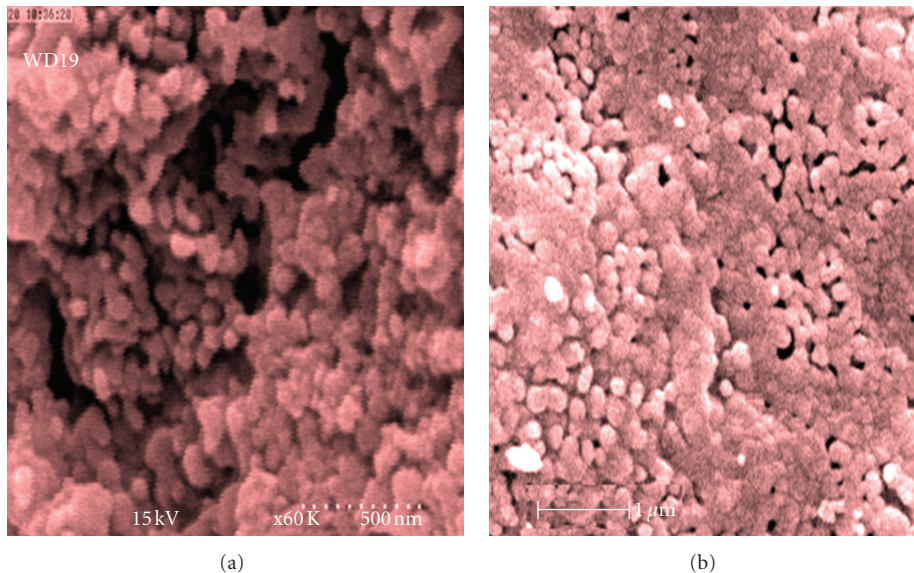


FIGURE 5: Scanning electron microscopy (SEM) of ZnO nanoparticle (a) and adsorbed dye on ZnO film (b).

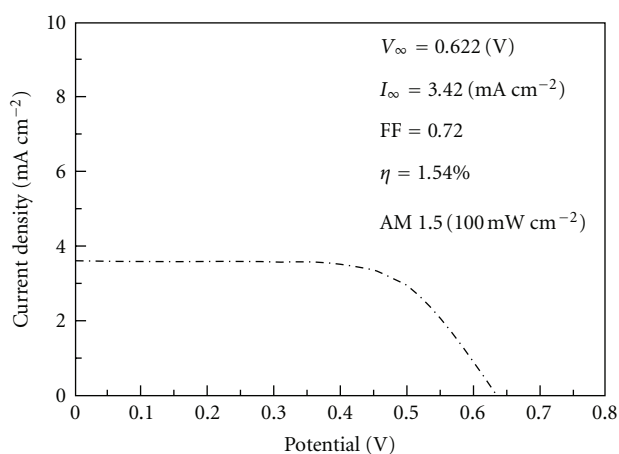


FIGURE 6: Typical photocurrent-voltage curve for the $(\text{Ru}(\text{phen})_2(\text{phendione}))^{2+}$ (1) sensitized ZnO solar cell under the standard AM 1.5 irradiation (100 mW cm^{-2}). η is 1.54% with J_{sc} of 3.42 mA cm^{-2} , V_{oc} of 0.622 V, and ff of 0.72.

isonicotinic acid, deeb is 4,4'-(CO₂Et)₂-2,2'-bipyridine, deeb is 4,4'-(CO₂Et)₂-bpy, and dcb-H₂ is 4,4'-(CO₂H)₂-bpy. $(\text{Ru}(\text{phen})_2(\text{phendione}))\text{PF}_6$ (1) sensitizer converts visible light at 400–500 nm to current with a maximum efficiency of 38% at 485 nm. To compare the IPCE between Ru phendione complexes and the same structures, it is useful to note that the Qu et al. [37] reported the photocurrent action spectra of TiO₂ surfaces pretreated at pH = 1, 2, 5, and 11 sensitized with $\text{Ru}(\text{deeb})-(\text{bpy})_2^{2+}$ in either 0.5 M TBAI/0.05 M I₂ or 0.5 M LiI/0.05 M I₂ acetonitrile electrolyte. With TBAI/I₂, the pH = 1 and pH = 2 acid-pretreated surfaces demonstrated high incident IPCE 45% and 70%, respectively, while the pH = 5 and pH = 11 pretreated samples gave very small IPCE 4% and 2%, respectively. With LiI in the electrolyte, the IPCE of pH = 5 and pH = 11 pretreated TiO₂ was dramatically

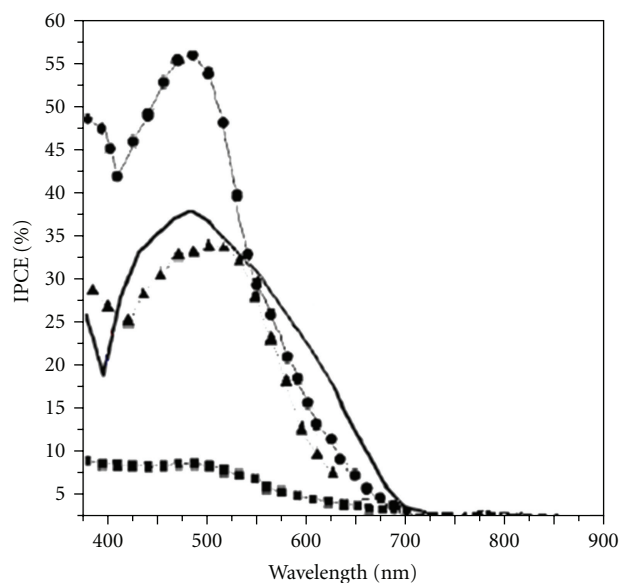


FIGURE 7: Photocurrent action spectrum obtained with the nanocrystalline ZnO solar cell sensitized by $(\text{Ru}(\text{phen})_2(\text{phendione}))^{2+}$ (1) with the electrolyte of 0.6 M DMPImI, 0.1 M LiI, 0.05 M I₂, and 0.5 M TBPA in methoxyacetonitrile (solid line) and $\text{Ru}(\text{deeb})(\text{bpy})_2^{2+}/\text{TiO}_2$ in 0.5 M LiClO₄/0.05 M I₂ electrolyte. The TiO₂ surfaces were pretreated with pH 2 (circles) aqueous solution [37]. $\text{Ru}-(\text{deeb})_2(\text{py})_2/\text{TiO}_2$ (squares) and $\text{Ru}(\text{bpy})_2(\text{ina})_2/\text{TiO}_2$ (triangles) are regenerative solar cell in 0.5 M LiI/0.05 M I₂ acetonitrile electrolyte [38]. IPCE is represented as a function of wavelength.

improved, 54% and 27%, respectively. The IPCE for the pH = 1 and pH = 2 pretreated samples is also high as 30% and 57%, respectively. Photocurrent action spectra, for $\text{Ru}(\text{bpy})_2(\text{ina})_2/\text{TiO}_2$ and $\text{Ru}(\text{deeb})_2(\text{py})_2/\text{TiO}_2$ in a 0.5 M LiI/0.05 M I₂ acetonitrile electrolyte measured at room temperature, are calculated as 33% and 3%, respectively. So, in

comparison with our results, the IPCE decreased in the order $\text{Ru}(\text{dcb})(\text{bpy})_2/\text{TiO}_2 = \text{Ru}(\text{deeb})(\text{bpy})_2/\text{TiO}_2$ in low pH > Ru -phendione complexes/ ZnO > $\text{Ru}(\text{bpy})^{2-}(\text{ina})_2/\text{TiO}_2$ > $\text{Ru}(\text{deeb})_2(\text{py})_2/\text{TiO}_2$.

As mentioned in Table 2, the best performance for ruthenium complexes with noncarboxylic acid was obtained with phosphonic terpyridine complexes with IPCE values up to 70%; these appear to be promising candidates to compete with carboxylated analogous [49]. These new photosensitizers exhibit intense, broad MLCT absorption, covering a wide range of visible light.

The rate of electron transport in Ru phendione complexes is a major element of the overall efficiency of the cells. The electrons, injected into the conduction band from optically excited complex, can traverse the ZnO network and be collected at the transparent conducting glass or can react with a redox mediator. The reaction of conduction band electrons with a redox mediator gives undesirable dark currents reducing significantly the charge-collection efficiency and thereby decreasing the total efficiency of the cell. The binding coordination of the complex on the ZnO and TiO_2 surfaces is almost the same [10, 11]. Photovoltaic performance of the $\text{Ru}(\text{dcbpy})_2(\text{NCS})_2/\text{ZnO}$ (where the ligand $\text{dcbpy} = 4,4'$ -dicarboxy-2,2'-bipyridine) solar cell is inferior to that of the $\text{Ru}(\text{dcbpy})_2(\text{NCS})_2/\text{TiO}_2$ solar cell [50–52].

To obtain clear view about limitations and advantages of Ru phendione complexes/ ZnO rather than the other dyes/semiconductors, it is important to note that dependence of photocurrent performance on semiconductor materials, $\text{TiO}_2 > \text{ZnO} > \text{SnO}_2 > \text{In}_2\text{O}_3$ [10, 11], is mainly due to two suggested cases, first, differences in the conduction band levels of semiconductors, and/or second, the aggregation of dye on the semiconductor electrode. [51, 53]. In the first case, Asbury et al. [53] observed much slower electron injection from $\text{Ru}(\text{dcbpy})_2(\text{NCS})_2$ in ZnO compared to that in TiO_2 by femtosecond mid-IR absorption spectroscopy. They suggested that different electron injection kinetics in $\text{Ru}(\text{dcbpy})_2(\text{NCS})_2/\text{ZnO}$ and $\text{Ru}(\text{dcbpy})_2(\text{NCS})_2/\text{TiO}_2$ solar cells may be due to the difference in electronic coupling between the π^* orbital of the dye and accepting orbital in ZnO and TiO_2 and/or their density of states. The states near the conduction band edge of ZnO consist of 4s orbitals of Zn^{2+} , while those of TiO_2 consist of 3d orbitals of Ti^{4+} , resulting in a difference in electronic coupling with the π^* orbital of the dye.

In the second, based on literature [51], protons derived from the Ru-complexes containing carboxylic acid groups make the dye-loading solution relatively acidic and dissolve ZnO, which generate Zn^{2+} /dye aggregates. Such aggregates are harmful to the cells, because they can reduce the electron injection efficiencies and fill nanoscale pores of the ZnO photoanodes.

Our data clearly indicate that phendione complexes as photosensitizers are adsorbed on ZnO nanoparticle and solve the problem of ZnO aggregation. We conclude that dye-phendione complexes, which neither produce solution acidic nor dissolve ZnO, are able to improve efficient electron injection into the semiconductor conduction band.

4. Conclusion

In summary, we fabricated a new binding state useful for attachment of Ru phendione complexes onto nanocrystalline ZnO surface. IR, UV-visible spectra, and AFM images supported favorable interfacial binding between the dye molecules, and ZnO, surface, the decrease IR absorption owing to the C=O stretch mode, and the effective red shift in UV-vis spectra in MLCT bands supported the formation of the chelating linkage on dye-anchored ZnO films. The Ru phendione complexes used in this study show suitable properties for solar energy conversion applications. The relatively improvement in the overall solar cell efficiency in the present work originates from a controlled dye-sensitization procedure thorough avoiding dye aggregation.

However, the overall efficiency is still much lower, due to lack of absorption in the visible and near IR regions. Thus, the challenges to reach the results reported on dye Ru carboxylated/ TiO_2 systems remain. Further work on phendione complexes is in progress, and we believe that improvement can be accomplished by a thorough replacement of attached functionalized groups to phendione complexes. Moreover, to fundamentally understand how differences in nanostructured films, for example, conductivity, affect the photoconversion efficiency, a more detailed investigation of different particle sizes, film thickness, and film morphology needs to be done.

Acknowledgments

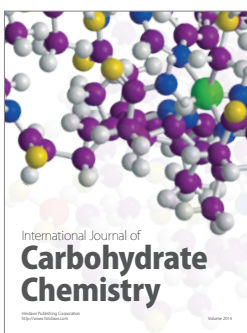
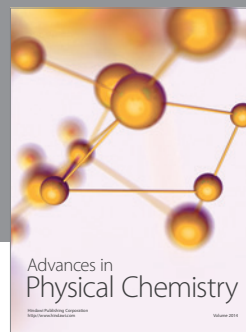
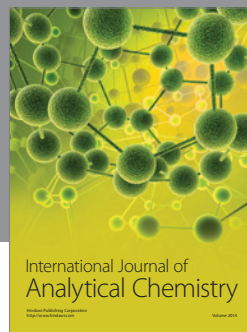
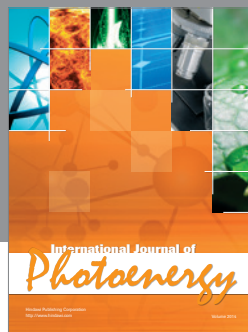
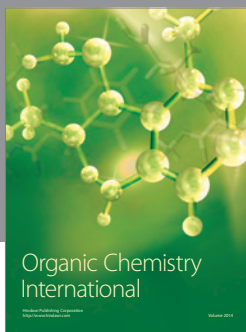
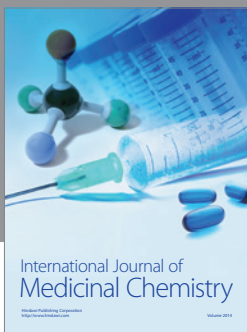
Thanks are extended to Professor K. Nazeeruddin from EPFL for proofreading the original manuscript and his useful comments. Also, the authors thank Zanjan University for financial supports and Laser Research Institute of Shahid Beheshti University for technical supports.

References

- [1] B. O'Regan and M. Grätzel, "A low-cost, high-efficiency solar cell based on dye-sensitized colloidal TiO_2 films," *Nature*, vol. 353, no. 6346, pp. 737–740, 1991.
- [2] M. Grätzel, "Photoelectrochemical cells," *Nature*, vol. 414, no. 6861, pp. 338–344, 2001.
- [3] M. K. Nazeeruddin, A. Kay, I. Rodicio et al., "Conversion of light to electricity by $\text{cis-X}_2\text{bis}(2,2'$ -bipyridyl-4,4'-dicarboxylate)ruthenium(II) charge-transfer sensitizers (X = Cl-, Br-, I-, CN-, and SCN-) on nanocrystalline TiO_2 electrodes," *Journal of the American Chemical Society*, vol. 115, no. 14, pp. 6382–6390, 1993.
- [4] C.-S. Chou, C.-M. Hsiung, C.-P. Wang, R.-Y. Yang, and M.-G. Guo, "Preparation of a counter electrode with p-type nio and its applications in dye-sensitized solar cell," *International Journal of Photoenergy*, vol. 2010, Article ID 902385, 9 pages, 2010.
- [5] G.-Y. Chen, M.-W. Lee, and G.-J. Wang, "Fabrication of dye-sensitized solar cells with a 3D nanostructured electrode," *International Journal of Photoenergy*, vol. 2010, Article ID 585621, 7 pages, 2010.
- [6] S. Ito, T. N. Murakami, P. Comte et al., "Fabrication of thin film dye sensitized solar cells with solar to electric power

- conversion efficiency over 10%," *Thin Solid Films*, vol. 516, no. 14, pp. 4613–4619, 2008.
- [7] E. Figgemeier and A. Hagfeldt, "Are dye-sensitized nanostructured solar cells stable? An overview of device testing and component analyses," *International Journal of Photoenergy*, vol. 6, no. 3, pp. 127–140, 2004.
- [8] M. Grätzel, "Dye-sensitized solar cells," *Journal of Photochemistry and Photobiology C*, vol. 4, no. 2, pp. 145–153, 2003.
- [9] Y.-C. Liu, Y.-F. Lu, Y.-Z. Zeng, C.-H. Liao, J.-C. Chung, and T.-Y. Wei, "Nanostructured mesoporous titaniumdioxide thin film prepared by sol-gel method for dye-sensitized solar cell," *International Journal of Photoenergy*, vol. 2011, Article ID 619069, 9 pages, 2011.
- [10] J. N. De Freitas, V. C. Nogueira, B. I. Ito et al., "Dye-sensitized solar cells and solar module using polymer electrolytes: stability and performance investigations," *International Journal of Photoenergy*, vol. 2006, Article ID 75483, 6 pages, 2006.
- [11] K. Hara, H. Sugihara, Y. Tachibana et al., "Dye-sensitized nanocrystalline TiO₂ solar cells based on ruthenium(II) phenanthroline complex photosensitizers," *Langmuir*, vol. 17, no. 19, pp. 5992–5999, 2001.
- [12] K. Kakiuchi, E. Hosono, and S. Fujihara, "Enhanced photoelectrochemical performance of ZnO electrodes sensitized with N-719," *Journal of Photochemistry and Photobiology A*, vol. 179, no. 1-2, pp. 81–86, 2006.
- [13] C. Bauer, G. Boschloo, E. Mukhtar, and A. Hagfeldt, "Electron injection and recombination in Ru(dcbpy)₂(NCS)₂ sensitized nanostructured ZnO," *Journal of Physical Chemistry B*, vol. 105, no. 24, pp. 5585–5588, 2001.
- [14] M. Law, L. E. Greene, J. C. Johnson, R. Saykally, and P. Yang, "Nanowire dye-sensitized solar cells," *Nature Materials*, vol. 4, no. 6, pp. 455–459, 2005.
- [15] K. Tennakone, P. V. V. Jayaweera, and P. K. M. Bandaranayake, "Dye-sensitized photoelectrochemical and solid-state solar cells: charge separation, transport and recombination mechanisms," *Journal of Photochemistry and Photobiology A*, vol. 158, no. 2-3, pp. 125–130, 2003.
- [16] A. B. F. Martinson, J. E. McGarrah, M. O. K. Parpia, and J. T. Hupp, "Dynamics of charge transport and recombination in ZnO nanorod array dye-sensitized solar cells," *Physical Chemistry Chemical Physics*, vol. 8, no. 40, pp. 4655–4659, 2006.
- [17] B. Cao, X. Teng, S. H. Heo et al., "Different ZnO nanostructures fabricated by a seed-layer assisted electrochemical route and their photoluminescence and field emission properties," *Journal of Physical Chemistry C*, vol. 111, no. 6, pp. 2470–2476, 2007.
- [18] L. E. Greene, M. Law, D. H. Tan et al., "General route to vertical ZnO nanowire arrays using textured ZnO seeds," *Nano Letters*, vol. 5, no. 7, pp. 1231–1236, 2005.
- [19] R. Könenkamp, K. Boedeker, M. C. Lux-Steiner et al., "Thin film semiconductor deposition on free-standing ZnO columns," *Applied Physics Letters*, vol. 77, no. 16, pp. 2575–2577, 2000.
- [20] H. Horiuchi, R. Katoh, K. Hara et al., "Electron injection efficiency from excited N₃ into nanocrystalline ZnO films: effect of (N₃-Zn²⁺) aggregate formation," *Journal of Physical Chemistry B*, vol. 107, no. 11, pp. 2570–2574, 2003.
- [21] M. Grätzel, "Conversion of sunlight to electric power by nanocrystalline dye-sensitized solar cells," *Journal of Photochemistry and Photobiology A*, vol. 164, no. 1–3, pp. 3–14, 2004.
- [22] B. Jing, H. Zhang, M. Zhang, Z. Lu, and T. Shen, "Ruthenium(II) thiocyanate complexes containing 4'-(4-phosphonatophenyl)-2,2',5',2''-terpyridine: synthesis, photophysics and photosensitization to nanocrystalline TiO₂ electrodes," *Journal of Materials Chemistry*, vol. 8, no. 9, pp. 2055–2060, 1998.
- [23] M. Li, Z. Xiao, Z. Huan, and Z. Lu, "New binding state useful for attachment of dye-molecules onto TiO₂ surface," *Applied Surface Science*, vol. 125, no. 2, pp. 217–220, 1998.
- [24] V. Aranyos, H. Grennberg, S. Tingry, S. E. Lindquist, and A. Hagfeldt, "Electrochemical and photoelectrochemical investigation of new carboxylatobipyridine (bis-bipyridine)ruthenium(II) complexes for dye-sensitized TiO₂ electrodes," *Solar Energy Materials and Solar Cells*, vol. 64, no. 2, pp. 97–114, 2000.
- [25] O. Schwarz, D. Van Loyen, S. Jockusch, N. J. Turro, and H. Dürr, "Preparation and application of new ruthenium(II) polypyridyl complexes as sensitizers for nanocrystalline TiO₂," *Journal of Photochemistry and Photobiology A*, vol. 132, no. 1-2, pp. 91–98, 2000.
- [26] Y. Yang, J. Tao, X. Jin, and Q. Qin, "New microporous polymer electrolyte based on polysiloxane grafted with imidazoliumiodide moieties for DSSC," *International Journal of Photoenergy*, vol. 2011, Article ID 405738, 9 pages, 2011.
- [27] S. A. Trammell, J. A. Moss, J. C. Yang et al., "Sensitization of TiO₂ by phosphonate-derivatized proline assemblies," *Inorganic Chemistry*, vol. 38, no. 16, pp. 3665–3669, 1999.
- [28] C. R. Rice, M. D. Ward, M. K. Nazeeruddin, and M. Grätzel, "Catechol as an efficient anchoring group for attachment of ruthenium-polypyridine photosensitizers to solar cells based on nanocrystalline TiO₂ films," *New Journal of Chemistry*, vol. 24, no. 9, pp. 651–652, 2000.
- [29] C. A. Goss and H. D. Abruna, "Spectral, electrochemical, and electrocatalytic properties of 1,10-phenanthroline-5,6-dione complexes of transition metals," *Inorganic Chemistry*, vol. 24, no. 25, pp. 4263–4267, 1985.
- [30] G. A. Shabir and N. J. Forrow, "Validation of a reversed-phase HPLC method for 1,10-phenanthroline-5,6-dione and analysis of its impurities by HPLC-MS," *Journal of Pharmaceutical and Biomedical Analysis*, vol. 33, no. 2, pp. 219–230, 2003.
- [31] F. Calderazzo, G. Pampaloni, and V. Passarelli, "1,10-Phenanthroline-5,6-dione as a building block for the synthesis of homo- and heterometallic complexes," *Inorganica Chimica Acta*, vol. 330, no. 1, pp. 136–142, 2002.
- [32] N. Margiotta, V. Bertolasi, F. Capitelli et al., "Influence of steric and electronic factors in the stabilization of five-coordinate ethylene complexes of platinum(II): X-ray crystal structure of [PtCl₂(2,9-dimethyl-1,10-phenanthroline-5,6-dione)]," *Inorganica Chimica Acta*, vol. 357, no. 1, pp. 149–158, 2004.
- [33] T. Fujihara, R. Okamura, T. Wada, and K. Tanaka, "Coordination ability of 1,10-phenanthroline-5,6-dione: syntheses and redox behavior of a Ru(II) complex with an o-quinoid moiety and of bridged Ru(II)-M(II) complexes (M = Pd, Pt)," *Dalton Transactions*, no. 16, pp. 3221–3226, 2003.
- [34] H. Shahroosvand, M. Khorasani-Motlagh, M. Noroozifar, M. Shabani, A. Fyezakhsh, and M. Abdouss, "Synthesis and characterisation of TiO₂ nanoparticle with polypyridily complexes for using in solar cells," *International Journal of Nanomanufacturing*, vol. 5, no. 3-4, pp. 352–365, 2010.
- [35] H. Shahroosvand, M. Khorasani-Motlagh, M. Noroozifar, M. Shabani, A. R. Fyezakhsh, and M. Abdouss, "Preparation and reactivity of MoO₂ nanoparticle based on polypyridily complexes," *Solid State Science in Proceedings of the 3rd Conference on Chemistry*, pp. 102, Islamic Azad University, Varamin-Pishva Branch, Varamin, Iran, 2008.
- [36] H. Shahroosvand, M. Shabani, M. Khorasani-Motlagh, and A. R. Fyezakhsh, "Synthesis and characterization of novel

- complexes of copper with polypyridyl ligands and TiO₂ nanoparticle for using solar cells,” in *Proceedings of the 2nd Conference on Nanostructures*, pp. 58–59, Kish Island, Iran, 2008.
- [37] P. Qu, D. W. Thompson, and G. J. Meyer, “Temperature-dependent electron injection from Ru(II) polypyridyl compounds with low lying ligand field states to titanium dioxide,” *Langmuir*, vol. 16, no. 10, pp. 4662–4671, 2000.
- [38] P. Qu and G. J. Meyer, “Proton-controlled electron injection from molecular excited states to the empty states in nanocrystalline TiO₂,” *Langmuir*, vol. 17, no. 21, pp. 6720–6728, 2001.
- [39] A. S. Polo, M. K. Itokazu, and N. Y. Murakami Iha, “Metal complex sensitizers in dye-sensitized solar cells,” *Coordination Chemistry Reviews*, vol. 248, no. 13–14, pp. 1343–1361, 2004.
- [40] H. Zabri, I. Gillaizeau, C. A. Bignozzi et al., “Synthesis and comprehensive characterizations of new cis-RuL₂X₂ (X = Cl, CN, and NCS) sensitizers for nanocrystalline TiO₂ solar cell using bis-phosphonated bipyridine ligands (L),” *Inorganic Chemistry*, vol. 42, no. 21, pp. 6655–6666, 2003.
- [41] J. Ohlsson, H. Wolpher, A. Hagfeldt, and H. Grennberg, “New dyes for solar cells based on nanostructured semiconducting metal oxides. Synthesis and characterisation of ruthenium(II) complexes with thiol-substituted ligands,” *Journal of Photochemistry and Photobiology A*, vol. 148, no. 1–3, pp. 41–48, 2002.
- [42] Y. Hou, P. Xie, K. Wu, J. Wang, B. Zhang, and Y. Cao, “Synthetic control of the photophysical and photoelectrochemical properties of ruthenium(II) polypyridyl complexes,” *Solar Energy Materials and Solar Cells*, vol. 70, no. 2, pp. 131–139, 2001.
- [43] T. A. Heimer, S. T. D’Arcangelis, F. Farzad, J. M. Stipkala, and G. J. Meyer, “An acetylacetonate-based semiconductor—sensitizer linkage,” *Inorganic Chemistry*, vol. 35, no. 18, pp. 5319–5324, 1996.
- [44] K. Kakiuchi, E. Hosono, and S. Fujihara, “Enhanced photoelectrochemical performance of ZnO electrodes sensitized with N-719,” *Journal of Photochemistry and Photobiology A*, vol. 179, no. 1–2, pp. 81–86, 2006.
- [45] J. B. Baxter, A. M. Walker, K. van Ommering, and E. S. Aydil, “Synthesis and characterization of ZnO nanowires and their integration into dye-sensitized solar cells,” *Nanotechnology*, vol. 17, no. 11, pp. 5304–5312, 2006.
- [46] K. Nakamoto, *Infrared and Raman Spectra of Inorganic and Coordination Compounds Part II: Application in Coordination, Organometallic and Bioinorganic*, John Wiley & Sons, New York, NY, USA, 1997.
- [47] C. Klein, M. K. Nazeeruddin, D. Di Censo, P. Liska, and M. Grätzel, “Amphiphilic ruthenium sensitizers and their applications in dye-sensitized solar cells,” *Inorganic Chemistry*, vol. 43, no. 14, pp. 4216–4226, 2004.
- [48] M. Hosokawa, K. Nogi, M. Naito, and T. Yokoyama, “A dye-sensitized solar cell utilizing metal nanoparticle,” in *Nanoparticle Technology Handbook*, chapter 5, pp. 438–439, Elsevier, 2007.
- [49] S. M. Zakeeruddin, M. K. Nazeeruddin, P. Pechy et al., “Molecular engineering of photosensitizers for nanocrystalline solar cells: synthesis and characterization of Ru dyes based on phosphonated terpyridines,” *Inorganic Chemistry*, vol. 36, no. 25, pp. 5937–5946, 1997.
- [50] H. Rensmo, K. Keis, H. Lindström et al., “High light-to-energy conversion efficiencies for solar cells based on nanostructured ZnO electrodes,” *Journal of Physical Chemistry B*, vol. 101, no. 14, pp. 2598–2601, 1997.
- [51] K. Keis, J. Lindgren, S. E. Lindquist, and A. Hagfeldt, “Studies of the adsorption process of Ru complexes in nanoporous ZnO electrodes,” *Langmuir*, vol. 16, no. 10, pp. 4688–4694, 2000.
- [52] G. Redmond, D. Fitzmaurice, and M. Graetzel, “Visible light sensitization by cis-bis(thiocyanato)bis(2,2’-bipyridyl-4,4’-dicarboxylato) ruthenium(II) of a transparent nanocrystalline ZnO film prepared by sol-gel techniques,” *Chemistry of Materials*, vol. 6, no. 5, pp. 686–691, 1994.
- [53] J. B. Asbury, Y. Wang, and T. Lian, “Multiple-exponential electron injection in Ru(dcbpy)₂(SCN)₂ sensitized ZnO nanocrystalline thin films,” *Journal of Physical Chemistry B*, vol. 103, no. 32, 1999.



Hindawi

Submit your manuscripts at
<http://www.hindawi.com>

